ISSN 2354-0575

ESTIMATION AND EXPERIMENTAL VERIFICATION OF WELDING TEMPERATURE BY GAS METAL ARC WELDING PROCESS

Ngo Thi Thao, Phan Ngoc Tuan, Than Van The
Hung Yen University of Technology and Education

Received: 08/12/2019
Revised: 10/3/2020
Accepted for publication: 22/3/2020

Abstract:

In this paper, the thermal model of butt joint in Gas Metal Arc Welding (GMAW) is constructed and simulated based on ANSYS software to obtain welding temperature field. Low carbon steel with temperature-dependent thermal properties due to very high welding temperature is considered. Volumetric heat source is determined through series equations for different welding conditions. Experiments are performed to measure and verify welding temperatures under different welding parameters. Results show that the simulation temperatures are in good agreement with the measurement temperatures for all cases. In addition, deformation and residual stress is also acquired through simulated results. This method strongly provides reliable information for finding an appropriate welding condition that will improve quality of welding products.

Keywords: *ANSYS, GMAW, Welding temperature, experiment..*

1. Introduction

Recently, numerical simulation has been widely applied in many welding technologies for finding an optimized condition which was a basis to select experimental welding conditions leading to reduce experiment times and price as well. ANSYS is a simulated tool for welding processes with many advantages; it was used for optimizing welding parameters to increase the life of the structure [1]. Residual strains in thin-walled circular seams of cylindrical shells using TIG butt welds was estimated using ANSYS simulation [2]. Ismail, M.I.S.a, and Afieq, W.M.a [3] have studied thermal analysis on a weld joint of aluminum alloy in GMAW (Gas metal arc welding) using finite element method. Most of these studies using ANSYS to build a computational model solved the thermal problem by writing code on ANSYS ADPL which is quite complex. While the application of ANSYS WORKBENCH in the simulation of welding processes, especially the molten welding, is very limited, and very few research has been published.

GMAW is commonly used in industry to join metals and these alloys. Narrow heat affected zone because of high concentration of heat source, low deformation, high welding efficiency, good protection, without using welding flux are the outstanding advantages of this welding method. Dongqing Yang et al. [4] have reported thermal analysis of single pass and multiple layer in the GMAW process using infrared thermography. An equivalent GTAW (Gas Tungsten Arc Welding) heat source was successfully estimated by Francois Pichot et al. [5]; they then conducted experiments to verify this result. Moreover, thermal analysis is very important to conduct the numerical simulation for welding process [6]. An application of finite element technique was used to simulate welding process presented in [7]. Goldak et al. [8] introduced a double ellipsoidal heat source model with Gaussian distribution of power density in space. There are many studies that successfully utilized the numerical simulation in the research and development of arc welding [9] and friction stir welding [10] which deal with the temperature field and weld bead geometry of welding by using numerical models. By carrying out the thermal analysis using the finite element method, the thermal field data could easily be acquired. However, it is not easy to determine the heat source in the molten weld zone due to many parameters affecting the process. Arshad Alam

SYED [11] has used a volumetric heat source for simulating the GMAW process. In his research, an analytically determined volumetric heat source was applied for butt welding joint.

In this paper, authors have calculated the heat source and successfully applied ANSYS WORKBENCH to model and simulate the temperature field, the stress and deformation for the butt welding joint in GMAW. After that, we conducted experiments to verify temperature results at some locations on the welding workpiece.

2. Thermal model of GMAW

A three –dimensional transient heat transfer analysis is used to simulate GMAW process with below governing and boundary equations [11]

$$\frac{\partial}{\partial x}\left(k(T)\frac{\partial T}{\partial x}\right)+\frac{\partial}{\partial y}\left(k(T)\frac{\partial T}{\partial y}\right)+\frac{\partial}{\partial z}\left(k(T)\frac{\partial T}{\partial z}\right)+q = \rho(T)C_p(T)\frac{\partial T}{\partial t} \quad (1)$$

$$k_n(T)\frac{\partial T}{\partial x}+h\left(T-T_0\right)+\sigma\varepsilon\left(T^4-T_0^4\right)=0 \quad (2)$$

where ρ, k and C_p are density, thermal conductivity and specific heat of workpiece material, respectively; t and T refer to time variable and temperature. n, k_n, h, ε,σ, and T_0 stand for normal direction to surface, thermal conductivity, heat transfer coefficient ($h=10W/m^2K$ [12]), emissivity, Stefan-Boltzmann constant, and the ambient temperature, respectively. In Eq. (1), q accounts for the arc heat input of a volumetric heat source given as Eq. (3)..

$$q=\frac{6\sqrt{3}f_iP\eta}{\pi\sqrt{\pi}a_ibc}\exp\left(-\frac{3x^2}{a_i^2}-\frac{3y^2}{b^2}-\frac{3z^2}{c^2}\right) \quad (3)$$

in which $P=\alpha UI$ is the arc power; α, I and U are efficiency coefficient, current and voltage. η is process efficiency. α and η are assigned at 0.75 and 0.8, respectively [13]. The subscript i indicates 1 and 2 corresponding to the front and rear heat sources. The volumetric heat source is considered as double semi-ellipsoids where a smaller semi- ellipsoid in front of the arc center and a larger semi- ellipsoid at the rear due to different heat transfer. a_1, a_2 , b and c are dimensions of semi major axes, minor axes and depths of the front and the rear semi-ellipsoids heat source. $a_1=f_1a$; $a_2=f_2a$; $c=\sqrt{\left[a^2-\left(a-a_1\right)^2\right]}$; and $b=(2a^3)/\left[(a_1+a_2)/c\right]$[11].

In this paper, ANSYS software is applied to model and simulate the GMAW process. The welding plates are designed and then imported to ANSYS for setting up boundary conditions. Fig. 1 shows the mesh of the entire plate that is finer at near welding center line and coarse in other regions. The SOLID90 (refer to Fig. 1.b) with higher order version of the 3-D eight node thermal element is utilized in the analysis. This element type is appropriate for analyzing thermal-mechanical case. The meshing model will herein help to save the computing time while ensuring accuracy of analyzed results. In addition, the material properties must be given attention because it exerts significant influence at high temperatures. In this work, the low carbon steel with temperature-dependent material properties including density, thermal conductivity and specific heat is considered. For moving heat source, it is assumed that speed is a constant along a welding line. The heat source is distributed in the corresponding to welding area of each step. Entire simulation process in ANSYS is summarized and demonstrated in Fig. 2

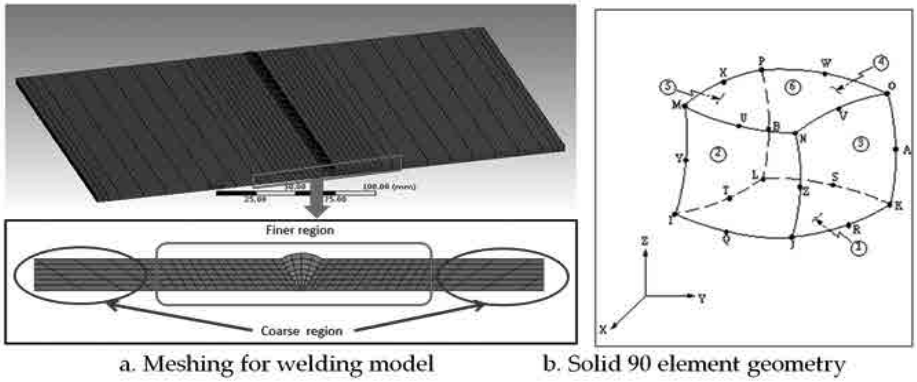

Fig. 1. Meshed model

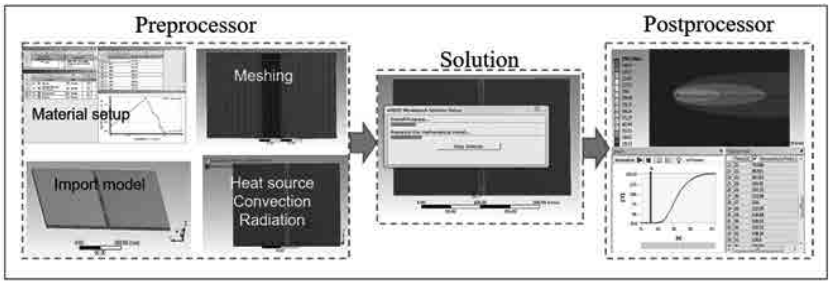

Fig. 2. Flowchart of simulation process in ANSYS

3. Experiment

An experimental setup schematic is shown in Fig. 3. In this study, the GMAW process was operated by a Miller MigMatic 380 DX-USA welding machine to weld a butt joint of steel workpiece with ϕ1 mm wire electrode under a shielding gas of CO_2. An auto welding carriage was used to carry welding torch for maintaining the given welding velocity and ensuring the welding quality. The steel workpiece size used in the experiments is 150 x 235 x 6 mm. The butt joint with 15^0 chamfer for each side which is put on a plate and no-restrain is prepared during welding process.

A portable data acquisition module (USB-4718) is used to record temperature data which is measured by five K-thermocouples at five positions on the sample. The locations of the five thermocouples in the welding sample are listed in Table 1. The USB-4718 is connected to a computer for displaying the temperature varying with time. The welding conditions were selected in this article as listed in Table 2.

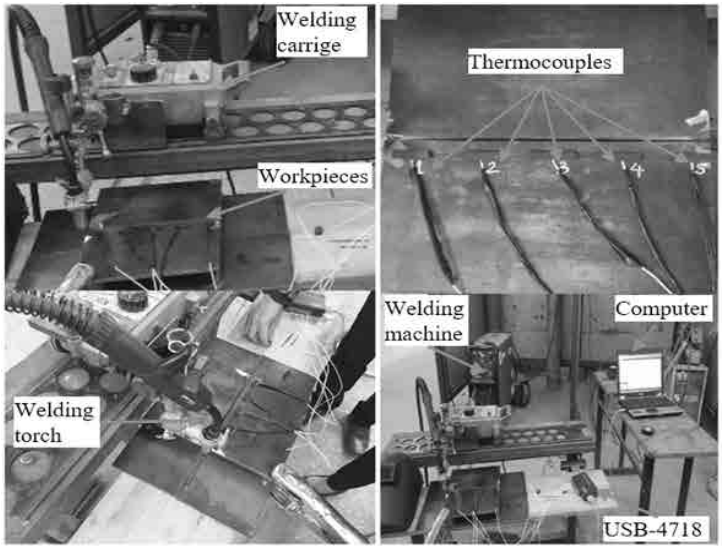

Fig. 3. Experiment setting

Table 1. Positions of thermocouple in welding workpiece

Positions	Sensor 1 (Ch1_m)	Sensor 2 (Ch2_m)	Sensor 3 (Ch3_m)	Sensor 4 (Ch4_m)	Sensor 5 (Ch5_m)
	From welding center line (mm)				
1st experiment	30	30	30	30	30
2nd experiment	15	15	10	15	15
3rd experiment	20	15	15	15	20
From start welding workpiece	25	70	125	175	220

Table 2. Simulation and experiment welding conditions

Welding conditions	1st condition	2nd condition	3rd condition
Welding current I_h (A)	160	155	150
Welding voltage U_h (V)	20	20	19
Welding speed V_h (mm/s)	5	4.2	4.2

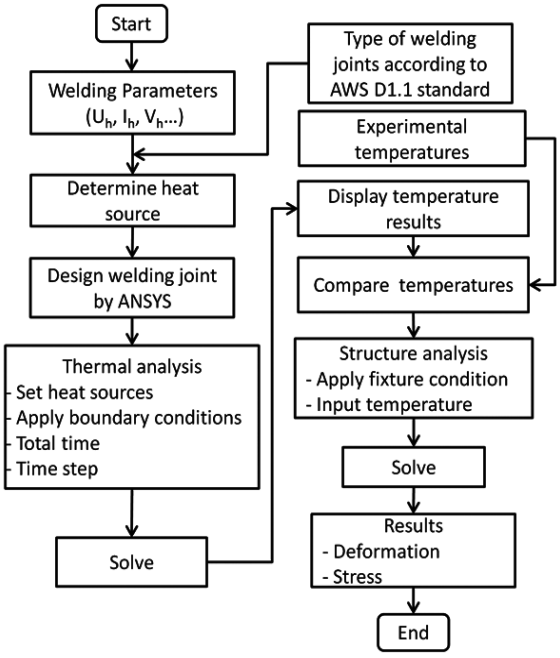

Fig. 4. Whole analysis process for welding problem

Measured temperatures on the welding workpiece are then compared with simulated temperature for verifying accuracy of proposed method. Results of deformation and stress are further obtained by solving structure problem. The whole process is summarized in Fig. 4.

4. Results and Discussions

4.1 Simulation results

Fig. 5 shows the distribution of temperature field on the welding specimen using the 1st welding condition. As observed, the temperature fields as well as the isothermal distributions on the welding part are clearly seen in the welding direction during the welding process. As seen, the maximum temperatures are about 1763.5 ^oC and 1734.3 ^oC at 1s and 2s, respectively. While temperature at 10s to 24s is maintained about 1803 ^oC. It can be due to unstable arc at beginning; when the arc is stable, the welding temperature becomes steady state. At the end of the weld due to excessive heat and less heat dissipation area, the temperature has jumped to 2121.7 ^oC as seen in Fig. 5. As observed, direction of heat transfer can be shown and the temperature field was extended toward welded part because of different heat transfer rate in the welding samples.

Fig. 6 indicates the welding temperatures along welding direction at intermediate welding times (10s, 30s, and 52s) under the 2nd condition. With the same welding speed and lower welding current, the welding temperature under 3rd condition is less than that under the 2nd condition (welding temperature at 1891.7^{0}C of the 3rd condition compared to 1978.7^{0}C of the 2nd condition as seen in Fig.7 and Fig.6, respectively).

In present work, the deformation and stress can be further acquired based on simulation temperatures. Fig. 8 depicts total deformation and equivalent stress distribution of the workpieces after welding under different conditions. The maximum magnitude of total deformations for three cases are about 0.4156mm, 0.45565mm, and 0,45212mm at the end of welding line. While the maximum equivalent stresses of 415.59MPa, 422.23MPa, and 418.33MPa are achieved along welding centerline. In addition, both distortion and stress are symmetrically distributed through the center of the weld. It can be seen that the maximum deformation and equivalent stress of the 2nd welding condition are higher than that of the 1st welding condition; the reason may be due to higher temperature made by the 2nd welding condition.

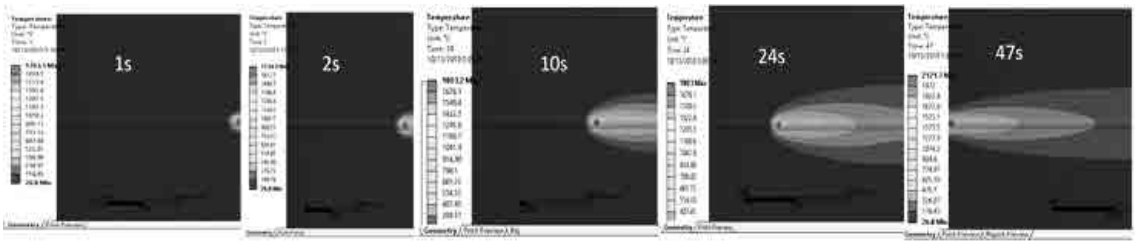

Fig. 5. Temperature distributions in welding workpiece using 1st condition

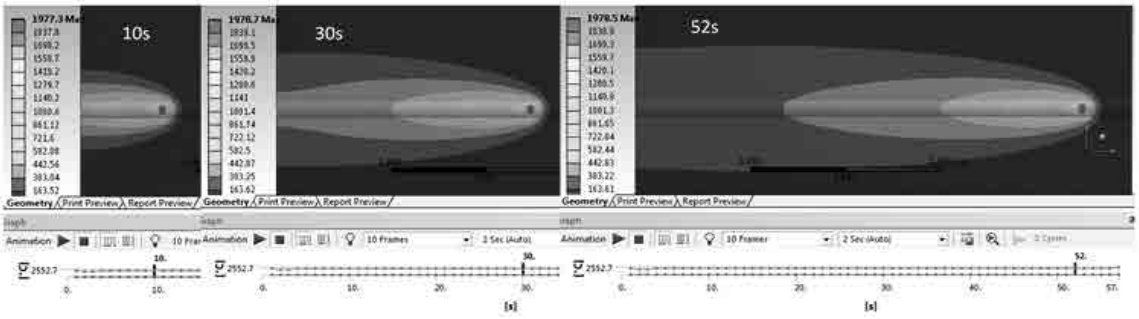

Fig. 6. Temperature distributions in welding workpiece using 2nd condition

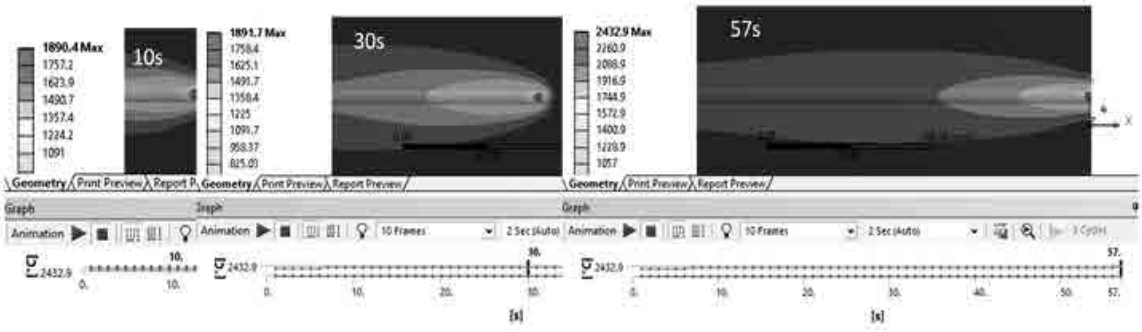

Fig. 7. Temperature distributions in welding workpiece using 3rd condition

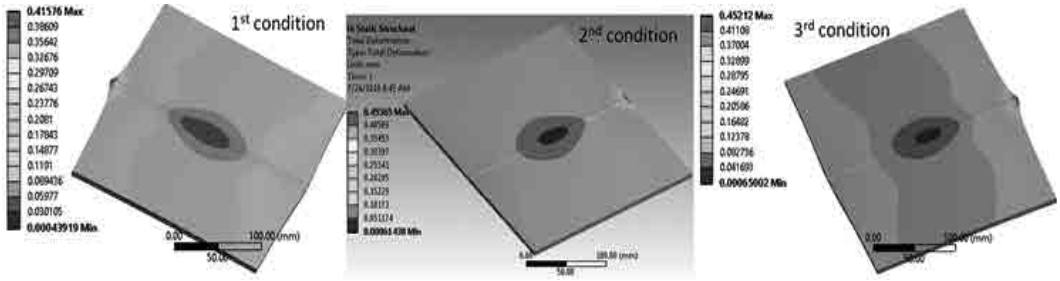

a. Total deformation

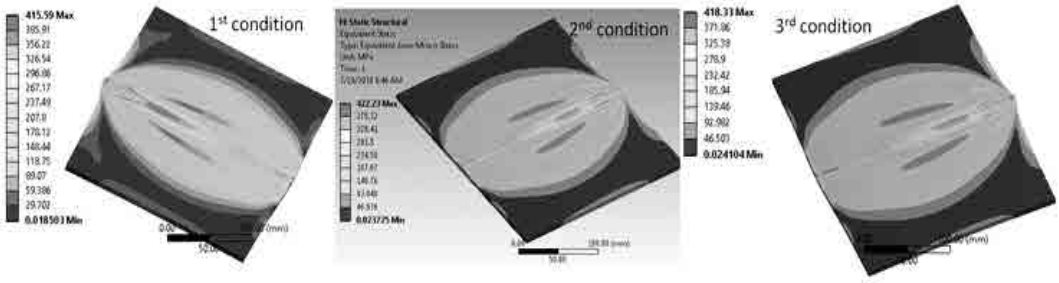

b. Stress

Fig. 8. Deformation and stress in welding workpiece under different conditions

Through simulated results, we can clearly estimate distribution of welding temperature along welding direction and distribution of total deformation as well as equivalent stress for the different welding conditions. Table 3 collects results of stable welding temperature, maximum total deformation and maximum equivalent stress. From the table, it shows that the welding temperature of 2nd and 3rd conditions is higher than that of 1st condition. This is because of the welding speed of

2nd and 3rd conditions lower than that of condition 1. The 2nd and 3rd conditions have the same speed. However, the welding temperature of 2nd condition is higher than that of 3rd condition. It is due to current of 2nd condition (155A) higher than current of 3rd condition (150A). The difference in the peak temperatures of these two conditions is about 87°C. Hence, it indicates that maximum temperature increases with increasing current. The simulation temperatures are then verified by experimentally measured temperature which will be presented in next section.

Table 3. Simulation results under different welding conditions

Simulation results	1st condition	2nd condition	3rd condition
Stable welding temperature (°C)	1803	1978	1891.3
Max. total deformation (mm)	0.4156	0.45565	0.45212
Max. equivalent stress (MPa)	415.59	422.23	418.33

4.2. Verification of welding temperature

In order to validate the accuracy of thermal analysis, simulated temperatures were compared with experimental temperatures at some locations in the workpiece. The temperature data for each thermocouple was recorded with respect to time during welding for three above welding conditions. As shown in Fig. 9a, the simulated temperatures agree well with the measured temperatures at all measurement positions under the 1st welding condition. The predicted results were slightly higher than experimental results because of a small amount heat lost due to transfer to welding fixture. Similarly, the 2nd welding condition is used to measure temperature at other measurement locations. A comparison of simulated and experimental temperature is illustrated in Fig. 9b. Clearly, the highest temperature was found at thermocouple 3 placed closest to welding center line. An agreement between the experimental and numerical results was also observed in Fig. 9b. Fig. 9c indicates a comparison of estimated and measured temperatures with the 3rd welding condition at five other locations. A consistence of both trend and value of results were seen in Fig. 9c. The simulated temperatures matched well with measured temperatures. It can be said that simulation conditions and experimental conditions of selecting and setting heat source as well as boundary conditions are highly appropriate. From all results, one can say that the presented thermal model of GMAW can accurately predict welding temperatures.

5. Conclusions

ANSYS software is successfully applied to estimate welding temperature, stress and deformation in GMAW process. The low carbon steel butt joints were experimentally welded under given welding conditions. Five thermocouples were embedded in the workpiece to record temperature at five points during welding process for three cases. The measured temperatures agree well with simulated temperatures for each welding condition. Results show that the welding temperature increases with decreasing speed; and, the welding temperature increases with raising the current. The verification of temperatures shows that the conditions setting in the proposed simulation process are similar to that in the experiments. Moreover, the predicted deformation and stress are also obtained through simulation results. Hence, the present method may provide some important information for easy selection of the reasonable welding conditions not only in GMAW but also in other welding processes to give high welding quality.

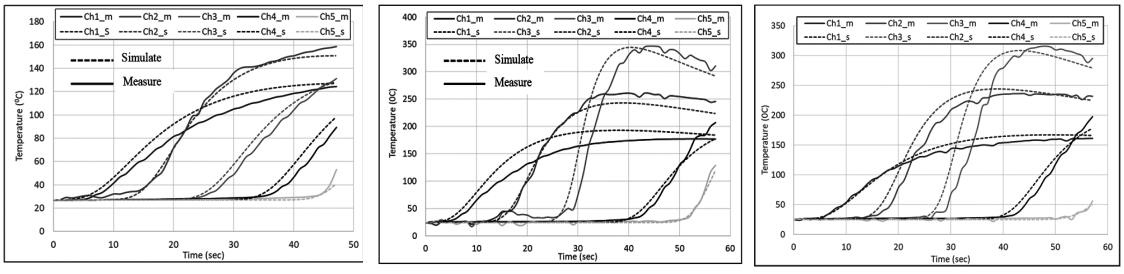

a. The 1st condition *b. The 2nd condition* *c. The 3rd condition*

Fig. 9. Comparison of simulated and experimental temperatures

References

[1]. Anuj Mehta, Khushal Diddee, Riyaz Mustufa, Ojus Jain Experimental Study to Increase the Life of Welding Nozzle. *IOSR Journal of Mechanical and Civil Engineering* **13**: 05-09, 2016.
[2]. A. Atroshenko , A. Vairis , V. Bichkov and R. Nikiforov, ANSYS Simulation of Residual Strains in Butt-welded Joints, *Journal of Engineering Science and Technology Review* **7 (5)**: 9-11, 2014.
[3]. Ismail M.I.S, Afieq W.M, Thermal analysis on a weld joint of aluminium alloy in gas metal arc welding. *Advances in Production Engineering & Management* **11 (1)**: 29–37, 2016.
[4]. Dongqing Yang, Gang Wang, Guangjun Zhang, Thermal analysis for single-pass multi-layer GMAW based additive manufacturing using infrared thermography. *Journal of Materials Processing Technology* **244**: 215–224, 2017.
[5]. Francois Pichot, Michel Danisa, Eric Lacoste, Yann Danis, Numerical definition of an equivalent GTAW heat source. *Journal of Materials Processing Technology* **213**: 1241– 1248, 2013.
[6]. Ma, J., Kong, F., Kovacevic, R., Finite-element thermal analysis of laser welding of galvanized high-strength steel in a zero-gap lap joint configuration and its experimental verification. *Materials & Design* **36**: 348-358, 2012.
[7]. Ueda, Y., Yamakawa, T., Analysis of thermal-elastic stress and strain during welding by finite element method. *Transactions of the Japan Welding Society* **2(2)**: 90-100, 1971.
[8]. Goldak, J., Chakravarti, A., Bibby, M., A new finite element model for welding heat sources. *Metallurgical Transactions B* **15(2)**: 299-305, 1984.
[9]. Long, H., Gery, D., Carlier, A., Maropoulos, P.G., Prediction of welding distortion in butt joint of thin plates. *Materials & Design* **30(10)**: 4126-4135, 2009.
[10]. Al-Badour, F., Merah, N., Shuaib, A., Bazoune, A. Thermo-mechanical finite element model of friction stir welding of dissimilar alloys. *The International Journal of Advanced Manufacturing Technology* **72(5-8)**: 607-617, 2014.
[11]. Arshad Alam SYED, Andreas PITTNER, Michael RETHMEIER, Amitava DE, Modeling of Gas Metal Arc Welding Process Using an Analytically Determined Volumetric Heat Source. *ISIJ International* **53**: 698–703, 2013.
[12]. Yilbas, B.S., Akhtar, S., Shuja, S.Z., Laser forming and welding processes. *Springer*, New York, 2013, doi: 10.1007/ 978-3-319-00981-0.
[13]. N. Pepe, S. Egerland, P. A. Colegrove, D. Yapp, A. Leonhartsberger and A. Scotti, Measuring the process efficiency of controlled gas metal arc welding processes. *Sci. Technol. Weld. Join.* **16(5)**: 412-417, 2011.

DỰ ĐOÁN VÀ KIỂM NGHIỆM NHIỆT ĐỘ HÀN SỬ DỤNG PHƯƠNG PHÁP HÀN HỒ QUANG ĐIỆN CỰC NÓNG CHẢY TRONG MÔI TRƯỜNG KHÍ BẢO VỆ

Tóm tắt:

Trong nghiên cứu này mô hình nhiệt của liên kết hàn giáp mối bằng phương pháp hàn hồ quang điện cực nóng chảy trong môi trường khí bảo vệ (GMAW) được xây dựng và mô phỏng dựa trên phần mềm ANSYS để nhận được trường nhiệt độ. Vật liệu thép cacbon thấp với các đặc tính nhiệt phụ thuộc vào nhiệt độ được xem xét. Nguồn nhiệt thể tích được xác định thông qua các phương trình cho các chế độ hàn hàn khác nhau. Các thí nghiệm được thực hiện để đo và kiểm chứng nhiệt độ hàn mô phỏng cho thông số chế độ hàn khác nhau. Kết quả cho thấy nhiệt độ mô phỏng phù hợp tốt với nhiệt độ đo cho tất cả các trường hợp. Ngoài ra, biến dạng và ứng suất dư cũng được sự đoán thông qua kết quả mô phỏng. Phương pháp này cung cấp các thông tin đáng tin cậy để có thể tìm một bộ thông số chế độ hàn thích hợp giúp nâng cao chất lượng kết cấu hàn.

Từ khóa: *ANSYS, GMAW, Nhiệt độ hàn, thực nghiệm.*